Development 128, 3001-3015 (2001)
Printed in Great Britain © The Company of Biologists Limited 2001
DEV8797

ribbon encodes a novel BTB/POZ protein required for directed cell migration in *Drosophila melanogaster*

Pamela L. Bradley and Deborah J. Andrew*

Department of Cell Biology and Anatomy, The Johns Hopkins University School of Medicine, 725 N. Wolfe Street, Baltimore, Maryland 21205-2196, USA
*Author for correspondence (e-mail: dandrew@jhmi.edu)

Accepted 7 May 2001

SUMMARY

During development, directed cell migration is crucial for achieving proper shape and function of organs. One well-studied example is the embryonic development of the larval tracheal system of *Drosophila*, in which at least four signaling pathways coordinate cell migration to form an elaborate branched network essential for oxygen delivery throughout the larva. FGF signaling is required for guided migration of all tracheal branches, whereas the DPP, EGF receptor, and Wingless/WNT signaling pathways each mediate the formation of specific subsets of branches. Here, we characterize *ribbon*, which encodes a BTB/POZ-containing protein required for specific tracheal branch migration. In *ribbon* mutant tracheae, the dorsal trunk fails to form, and ventral branches are stunted; however, directed migrations of the dorsal and visceral branches are largely unaffected. The dorsal trunk also fails to form when FGF or Wingless/WNT signaling is lost, and we show that *ribbon* functions downstream of, or parallel to, these pathways to promote anterior-posterior migration. Directed cell migration of the salivary gland and dorsal epidermis are also affected in *ribbon* mutants, suggesting that conserved mechanisms may be employed to orient cell migrations in multiple tissues during development.

Key words: Directed migration, Trachea, Salivary gland, Wingless, EGF receptor, MAPK, *Drosophila melanogaster*

INTRODUCTION

Organ formation is a highly regulated process during which groups of cells coordinately reorganize into specific three-dimensional forms. Cell migration is an essential aspect of organ formation and involves not only cell movement, but movement in a specific direction at the correct time. Formation of the highly elaborate branched network of the *Drosophila* tracheal system is driven by cell shape changes, cell rearrangements and directed cell migration, and provides an excellent system in which to study these events (Manning and Krasnow, 1993; Samakovlis et al., 1996). The trachea forms from ten bilaterally paired placodes of approximately 80 cells each located along the ventrolateral surface of the embryo. Tracheal cells invaginate from these ectodermal placodes to form individual cellular sacs, from which the primary branches arise. Directed migration of the five primary branches, plus subsequent branching and fusion, results in a complex tubular network which supplies all larval tissues with oxygen.

Genetic analysis of mutations affecting tracheal formation has revealed the roles of many genes (reviewed by Affolter and Shilo, 2000). The bHLH-PAS transcription factor encoded by *trachealess* (*trh*) is involved in the initial invagination step; in *trh* mutants all tracheal precursor cells remain at the embryo surface. The POU-domain transcription factor CF1a, encoded by *ventral veinless/drifter* (*vvl*/*dfr*), is also required early in tracheogenesis. TRH and VVL regulate known target genes necessary for the internalization of the primordia and subsequent branching events (see also figure 5 in Boube et al., 2000). Once internalized, the Fibroblast growth factor (FGF) homologue Branchless (BNL) and its receptor Breathless (BTL) are essential for primary branch formation; mutations affecting either molecule result in a fully internalized, but unelaborated sac of tracheal cells (see Fig. 1). The BNL signal is expressed in target tissues towards which tracheal cells normally migrate, and BTL is expressed in tracheal cells. Transduction of the BNL signal through BTL is thought to guide migration towards BNL sources.

In addition to the spatial guidance cues provided by BNL/BTL activity, at least three other signaling pathways have been implicated in primary branch formation: Decapentaplegic (DPP), Epidermal growth factor receptor (EGFR), and Wingless (WG)/WNT (see Fig. 1). DPP signaling is required to form the three branches that migrate along the dorsoventral axis: the dorsal branch (DB), the lateral trunk (LT), and the ganglionic branch (GB; Llimargas and Casanova, 1997; Vincent et al., 1997). DPP signaling in the dorsoventral branches activates expression of *knirps* (*kni*; Vincent et al., 1997), which encodes a transcription factor that mediates dorsoventral migration (Chen et al., 1998). EGFR signaling has an early role in invagination (Llimargas and Casanova, 1999) and is also reported to be involved in the migration of the dorsal

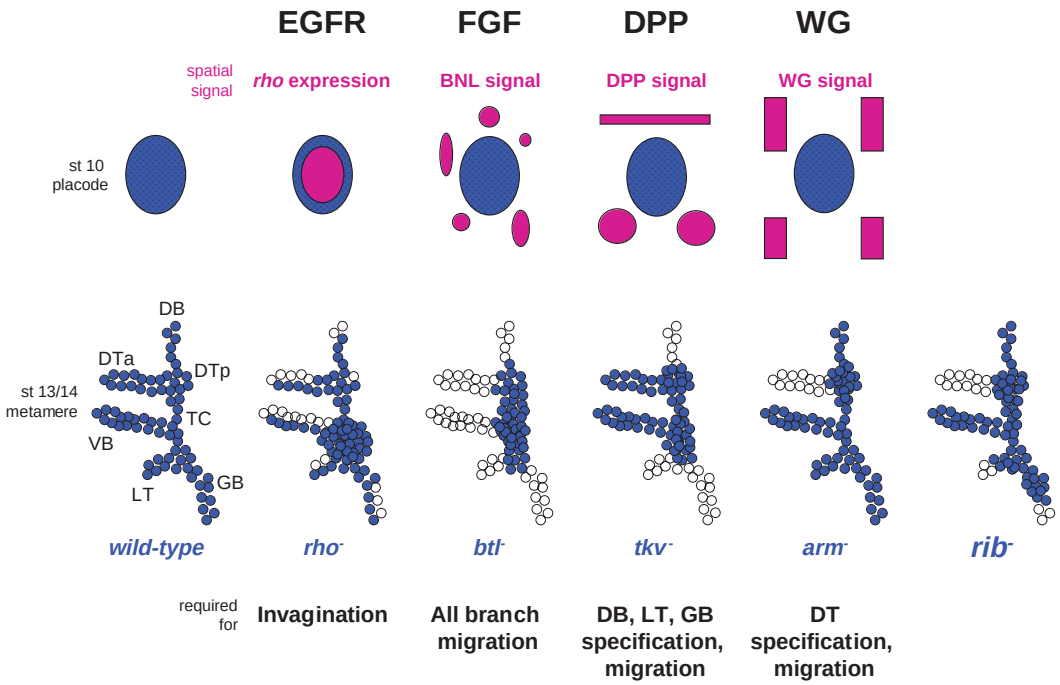

Fig. 1. Multiple signaling pathways are required for tracheal branching. The top half of the figure depicts tracheal placodes (blue) at embryonic stage 10 and the sources of activation (magenta) of four signaling pathways known to function during tracheogenesis (EGFR, FGF, DPP, WG). The lower portion of the figure depicts tracheal metameres at stage 13/14. By this stage, wild-type trachea have formed the five primary branches: dorsal branch (DB), dorsal trunk anterior and posterior (DTa, DTp), visceral branch (VB), lateral trunk (LT), and ganglionic branch (GB). TC, transverse connective. Defects in the components of the pathways are schematized (representative genotypes of the mutants are noted below each metamere). White circles represent absence of appropriately migrating tracheal cells in mutant metameres; blue circles represent the observed positions of the tracheal cells. EGFR signaling is initiated by a localized source of RHO within the placode (magenta; Bier et al., 1990). In the absence of EGFR signaling, many cells fail to invaginate and remain clustered on the surface of the embryo, and cells are missing from every branch (see also Fig. 3G-H′). The BNL/FGF ligand is expressed in patches outside the trachea (magenta) and signals to the BTL/FGFR, which is expressed in the tracheal placode. In the absence of FGF signaling, all branches fail to migrate. The DPP ligand has localized sources dorsal and ventral to the placode (magenta) and signals through the receptors TKV (expressed in the placode) and PUT (expressed ubiquitously; Affolter et al., 1994; Ruberte et al., 1995). *kni* expression is DPP-dependent in the DB, LT, and GB. In the absence of DPP signaling, *kni* expression is lost in the DB, LT and GB, and these branches do not form. WG is expressed adjacent to the tracheal placodes (magenta) and signals to the tracheal placode to direct the transcriptional activities of ARM and dTCF. One downstream target of WG signaling is *sal*. In the absence of WG signaling, *sal* expression is lost, and DT cells fail to migrate away from the transverse connective (TC). It should be noted that other WNT molecules may be required to activate signaling through ARM/dTCF since *arm* and *dTCF* mutant phenotypes are stronger than the *wg* phenotype alone (Llimargas, 2000). In embryos lacking *rib* function, no DT is formed and the LT and GB are stunted in their migration. Stages are according to Campos-Ortega and Hartenstein (Campos-Ortega and Hartenstein, 1985).

trunk (DT) and visceral branch (VB; Llimargas and Casanova 1997; Wappner et al., 1997). Also, WG/WNT signaling is required for DT formation (Chihara and Hayashi, 2000; Llimargas, 2000). These pathways play positive, instructive roles in the formation of specific branches, and also have antagonistic activities. For example, the *spalt* (*sal*) gene is initially expressed throughout the dorsal half of the tracheal placode and is subsequently restricted to the DT cells (Kuhnlein and Schuh, 1996). Spatial regulation of *sal* expression is achieved by EGFR and WG/WNT signaling, which activate *sal* expression (Wappner et al., 1997; Chihara and Hayashi, 2000; Llimargas, 2000), and by DPP signaling in the DB cells, which activates KNI, a direct transcriptional repressor of *sal* (Chen et al., 1998). Expression of *sal* in the DT is necessary for DT formation (Kuhnlein and Schuh, 1996), whereas loss of *sal* expression in the DB is necessary for DB formation (Chen et al., 1998).

Although these four signaling pathways (FGF, DPP, EGFR and WG/WNT) are required for normal tracheal development, it is not yet known how information from these pathways is integrated to promote the subcellular changes necessary for directed cell migration. Clearly, the identification and characterization of new mutations affecting tracheal development will reveal many of the events that underlie normal tracheogenesis and how information from signaling pathways is integrated and implemented.

Here, we describe a role for the *ribbon* (*rib*) gene in the directed migration of the tracheal DT cells. *rib* was first identified in the large-scale EMS mutagenesis screen for defects in cuticle structure (Nüsslein-Volhard et al., 1984). Subsequently, Jack and colleagues identified a role for *rib* in Malpighian tubule development, and described cell shape defects in several ectodermally derived tissues (Jack and Myette, 1997; Blake et al., 1998; Blake et al., 1999). We initially identified *rib* as a candidate mutant for a gene that was expressed in the trachea under the control of TRH. Although we proved that *rib* does not correspond to that nearby gene, we were intrigued by the phenotypes of *rib* mutant embryos. In this paper, we report defects in the early trachea and salivary glands of *rib* mutants and show that these organs fail to complete the directed movements needed to give rise to their final shapes. In the tracheal DT, loss of *rib* function most closely resembles loss of WG/WNT signaling, suggesting that *rib* may link this or other signaling pathways to the cellular changes necessary to undergo directed migration along the anteroposterior axis of the embryo. We also report the cloning of the *rib* gene and show that it encodes a novel BTB/POZ protein expressed widely during *Drosophila* embryogenesis.

Table 1. Antibodies used in this study

Antibody	Produced in	Dilution used	Reference	Source
Primary				
β-gal	Mouse (monoclonal)	1:10000	–	Promega
TRH	Rat	1:1000	Henderson et al., 1999	Our lab
DFR (VVL)	Rat	1:3000	Anderson et al., 1995	P. Israel-Johnson
KNI	Guinea pig	1:200	Kosman et al., 1998	D. Kosman
CRB	Mouse (monoclonal)	1:100	Wodarz et al., 1993	E. Knust/Hybridoma Bank
2A12	Mouse (monoclonal)	1:10	Patel, 1994	N. Patel/Hybridoma Bank
dpERK	Mouse (monoclonal)	1:1000	Gabay et al., 1997	Sigma
SAL	Rabbit	1:30	Kuhnlein et al., 1994	R. Schuh
dCREB-A	Rat	1:15000	Andrew et al., 1997	Our lab
DRI	Rat	1:15000	Gregory et al., 1996	R. Saint/our lab
Secondary				
Biotinylated guinea pig IgG	Goat	1:500	–	Vector Labs
Biotinylated mouse IgG	Horse	1:500	–	Vector Labs
Biotinylated rabbit IgG	Goat	1:500	–	Vector Labs
Biotinylated rat IgG	Rabbit	1:500	–	Vector Labs

MATERIALS AND METHODS

Fly strains

The wild-type fly strains used were Canton S (chromosomes) or Oregon R (embryos). The following strains were also used and are described in FlyBase (www.flybase.bio.indiana.edu): *Df(2R)P34*, *Df(2R)F7*, *Df(2R)*GC8, *Df(2R)GC10*, *cora*^{4}, *rho*$^{P\Delta 38}$, *rib*^{1}, *rib*^{2}, *sal*^{1}, *tkv*^{4}, *wbl*^{E4}, *wbl*^{RP}, *wbl*^{T6}, *wbl*^{M46}, *wbl*^{M88}, and *zip*^{1}. Two independent *wbl* genomic transgenes were tested for rescue (Konsolaki and Schupbach, 1998). The Gal4/UAS system (Brand and Perrimon, 1993), using the transgenes *UAS-sal* (Kuhnlein and Schuh, 1996) and *btl-Gal4* (Shiga et al., 1996), was used to express *sal* in all tracheal cells. The transgene *sal-TSE-lacZ* reports the tracheal expression of *sal* (Kuhnlein and Schuh, 1996). *rho-lacZ* R1.1 is an insertion in the *rho* gene that expresses *lacZ* in the same pattern as the endogenous *rho* transcript (Wappner et al., 1997). The *EP(2)2445* line (Rorth et al., 1998) contains a single P-element insertion at position 268,109 in Celera Genomics contig AE003796. A standard excision mutagenesis (Hamilton and Zinn, 1994) yielded two independent lethal lines, *EP(2)2445*$^{\Delta 1}$ and *EP(2)2445*$^{\Delta 2}$, that failed to complement *Df(2R)P34*. *UAS-rib* comprises a fragment spanning the coding region of *gene 5* which was amplified from the LD16058 cDNA by PCR and cloned into the pUAST expression vector (Brand and Perrimon, 1993). Germline transformation was performed as described previously (Rubin and Spradling, 1983) using *w*^{1118} embryos as the DNA recipients. Tracheal- and salivary gland (secretory cell)-specific rescue of *rib* defects was achieved using *btl-Gal4* or *fkh-Gal4* (Henderson and Andrew, 2000) to drive *UAS-rib*.

Antibodies, embryo staining and whole-mount in situ hybridizations

Embryo fixation and antibody staining were performed as described previously (Reuter et al., 1990). The antibodies used in this study are described in Table 1. Antibody-stained embryos were mounted on slides in methyl salicylate (Sigma). Whole-mount in situ hybridization to detect mRNA accumulation was performed using antisense digoxigenin-labeled RNA probes for hybridizations as described previously (Lehmann and Tautz, 1994), using the following cDNAs as templates: *bnl* (S. Hayashi), *btl* (D. Montell), *dpp* (W. Gelbart), *rib* (LD16058, Research Genetics), and *sal* (LD17463, Research Genetics). In situ hybridized embryos were mounted on slides in 70% glycerol to limit diffusion of the alkaline phosphatase reaction products. Homozygous mutant embryos were identified by morphological criteria, by the lack of β-gal staining, or by the lack of antisense *lacZ* hybridization. Staining with antibodies to β-gal, or *lacZ* hybridization, detects embryos carrying a balancer chromosome with a *lacZ* insert, specifically CyO-*ftz-lacZ* (CFL) or TM3-*Ubx-lacZ* (TUL). Embryos were visualized by Nomarski optics using a Zeiss Axiophot microscope. Ektar 25 or 100 print film (Kodak) was used for photography.

Cuticle preparations

Cuticles were prepared as described previously (Andrew et al., 1994), examined using both phase-contrast and dark-field optics, and photographed with TMAX 100 print film (Kodak).

Molecular analysis

BDGP cDNA clones (see Table 2) that mapped to unordered BACs in the 56C region were obtained from Research Genetics, sequenced, and grouped into genes. The genes were oriented relative to Celera Genomics clone AC020290, which was subsequently replaced by AE003797 and AE003796. The positions of these genes were mapped relative to local deficiency breakpoints by in situ hybridization to salivary gland polytene chromosomes, and was carried out according to procedures previously described (Pardue (1994) using the Vectastain kit (Vector Laboratories) for HRP signal detection, omitting the RNase treatment and acetylation steps.

The prediction programs Gene Finder (http://dot.imgen.bcm.tmc.edu:9331/gene-finder/gf.html) and GENSCAN (Burge and Karlin, 1997) were used to predict genes in the *rib* region. Predictions from these programs were compared with the sequences from the BDGP cDNA clones. In March 2000, annotated sequences for the entire region was released (Adams et al., 2000), which fully supported our molecular analysis.

Table 2. BDGP cDNAs used in this study

Gene	BDGP clot	BDGP ID	Celera ID
enb	396	SD09770	CG15112
1	14802	GH22187*	CG10737
	6321	LP04241	
2	4513	GH26057*	CG7097
	8632	GH01730	
	13764	SD01706	
	211	LD03454	
3	2582	LD19595*	CG7137
4	11792	GH13144*	CG7229
5	3448	LD16058*	CG7230
	10779	LD30267	
6	5610	LD27134	CG11906

*****cDNAs that were sequenced in their entirety on both strands as part of this analysis.

The RIB protein was analyzed by InterPro (http://www.ebi.ac.uk/interpro/), Pfam (http://pfam.wustl.edu), PROSITE (http://expasy.cbr.nrc.ca/prosite/), and PSORT (http://psort.nibb.ac.jp/form2.html). Homology searches were performed using BLAST (http://www.ncbi.nlm.nih.gov). Alignments were generated by CLUSTALX (Thompson et al., 1997) and illustrated using MacBoxshade (http://www.netaxs.com/jayfar/mops.html).

Sequence analysis of candidate ORFs in rib mutants

Two sources of template were used to amplify small overlapping regions of candidate gene ORFs by PCR: single embryos (*rib*/*rib*; selected for a lack of GFP expression from a *Kruppel-GFP* transgene on the CyO balancer chromosome (Casso et al., 1999) or genomic DNA isolated from heterozygous adult flies (*rib*/CFL). PCR with single embryos as template was performed as described previously (Franc et al., 1999). PCR products were sequenced and analyzed for allelic differences. All changes were verified by sequencing the corresponding regions on the opposite strand. DNA sequencing was performed at the Johns Hopkins University Core DNA Analysis Facility.

RESULTS

rib is required for specific directed cell migration in the trachea

rib mutants showed gross abnormalities in tracheal morphology at late stages (Fig. 2A,B), consistent with the phenotypes previously reported (Jack and Myette, 1997). To determine when defects were first apparent and if specific branches were affected, we examined *rib* mutant embryos using a panel of tracheal markers. Expression of three of the earliest expressed transcription factors, TRH, VVL/DFR and KNI, was completely normal at the placode stage, as was expression of two of their targets, *btl* and *rhomboid* (*rho*; Fig. 2C,D, and data not shown). These results indicated that specification of the tracheal primordia was unaffected in *rib* mutants. Moreover, there were no overt differences in the shape or size of tracheal placodes in *rib* mutants, and the invagination of tracheal cells was initiated with similar timing and positioning as in wild type. Differences were first apparent during stage 12, when outgrowth of branches was either absent or delayed (Fig. 2E,F). By stage 14, *rib* tracheae were clearly defective in a subset of branches (Fig. 2G,H). In most segments, the dorsal trunk was completely absent, and cells were clustered at the position within the tracheal sac from which DT cells normally migrate. In a few metameres, the cluster of DT cells in the trachea had fewer cells, and the corresponding DB contained additional cells. The LT and GB were also defective; both branches were stunted, and often the LT was completely absent. Unlike the DTs, which only rarely migrated, migrating GBs were frequently observed

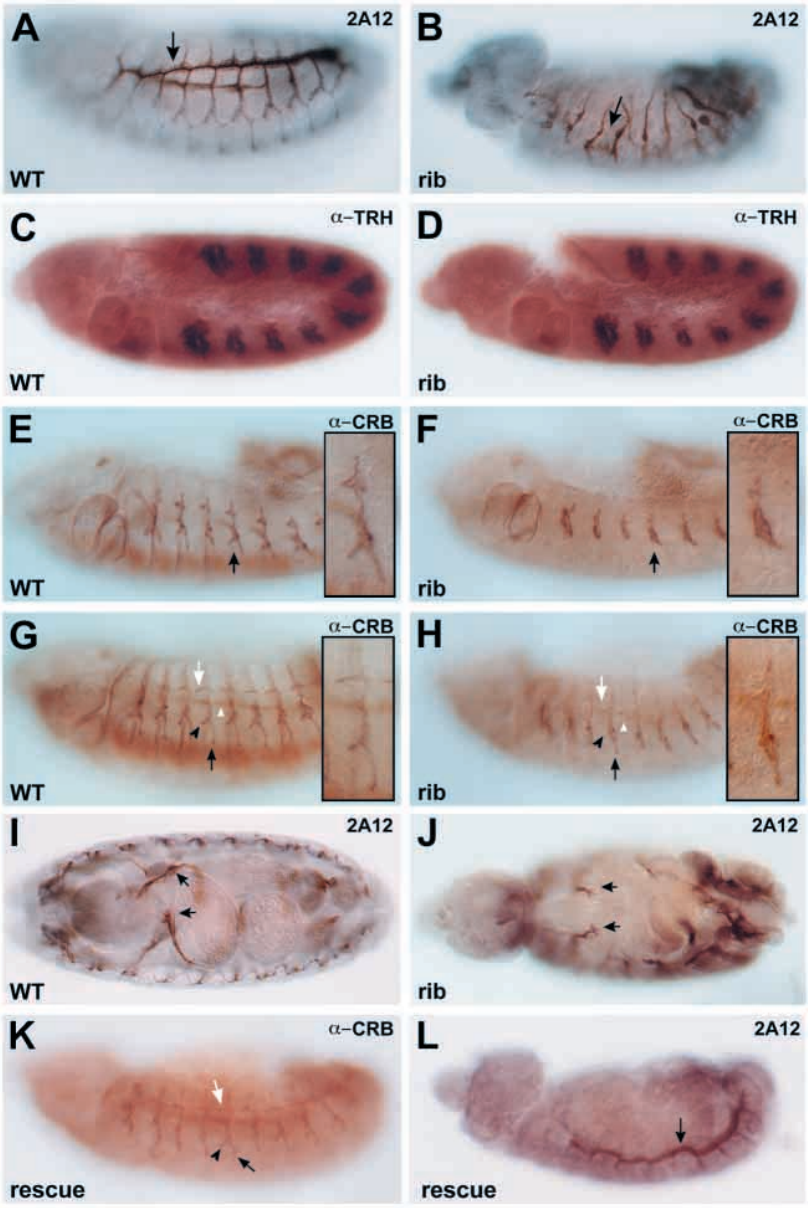

Fig. 2. *rib* mutants have defects in tracheal development. Embryos in the left column are wild-type; embryos in the right column are rib^1 homozygotes. A-H, K, and L are lateral views; I and J are dorsal views. 2A12 or anti-CRB was used to visualize the tracheal lumen, and anti-TRH to visualize nuclear TRH in all tracheal cells. The tracheal network is abnormal in rib^1 mutants (B). The most obvious difference is a complete loss of the main tracheal tube, the DT (arrow in B). The specification of tracheal placodes and early events of tracheal invagination appear normal in *rib* mutants (D). (E,F) By late stage 12, many of the tracheal branches in *rib* mutants have not migrated and lumen size is expanded (F), as compared with wild type (E). Insets in E,F,G,H are of metamere 4 (black arrow). (G,H) At stage 14, the DT (white arrow) is clearly absent in *rib* mutants (H) and the LT (black arrowhead) and GB (arrow) are stunted. The VB (white arrowhead) is visible out of the plane of focus (H). In late stage *rib* embryos (J), VBs reach the gut and perform terminal branching (arrows), as in wild type (I). (K,L) In embryos carrying *UAS-rib* and the tracheal driver *btl-Gal4*, tracheal phenotypes are rescued. (K) The lumina are less dilated, the two ventral branches are less stunted (black arrow and arrowhead), and DTs are migrating (white arrow). (L) Rescue of DT formation is obvious by late stages (arrow). On average, seven of the nine DT fragments form in these rescued embryos. Wild-type genotypes are rib^1/CFL, which were also stained with anti-βgal (brown staining in C,E,G), or Oregon R (A,I). No differences were observed in the phenotypes of embryos carrying one versus two wild-type alleles of *rib*.

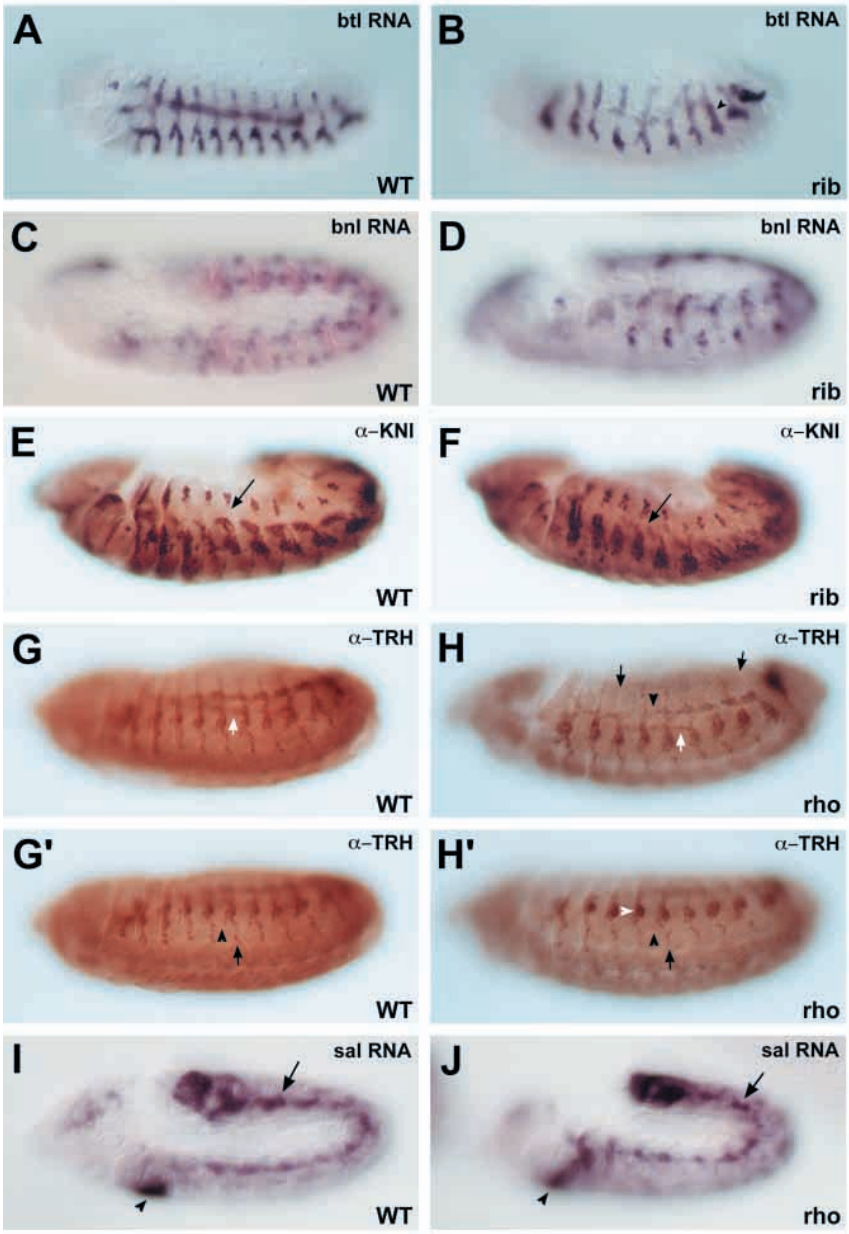

Fig. 3. *rib* does not function upstream of FGF, DPP or EGFR. All views are lateral. Stage 14 wild-type (A) and *rib*^{1} (B) embryos hybridized with an antisense *btl* RNA probe. *rib* mutants have similar expression, except that *btl* RNA expression is prolonged in TC cells (arrowhead; this difference is more obvious at earlier stages; not shown). Stage 11 wild-type (C) and *rib*^{1} (D) embryos hybridized with an antisense *bnl* RNA probe show similar expression patterns. Wild-type embryos were co-hybridized with a *btl* probe (pink staining in C). Stage 12 wild-type (E) and *rib*^{1} (F) embryos stained with anti-KNI have identical expression patterns; KNI is expressed in the DB, LT, and GB, and is lost from the TC and DT cells (arrow). Stage 14 wild-type (G,G′) or *rho*^{PΔ38} (H,H′) embryos stained with anti-TRH. *rho* embryos exhibit loss of several DBs (black arrows in H) and have fewer cells in the DT (arrowhead in H), LT (arrowhead in H′), and GB (arrow in H′), when compared with wild type. (Markings in G,G′ are identical to H,H′, except the view of the wild-type embryo in G is slightly more ventral than in H, placing the DBs out of the plane of focus.) A group of tracheal cells do not invaginate in *rho* mutants and are found in the same plane of focus as the epidermis (white arrowhead in H′). Early stage 12 wild-type (I) and *rho*^{PΔ38} mutant (J) embryos hybridized with an antisense *sal* probe show expression in the dorsal cells of tracheal pits (arrow). Embryos were co-hybridized with a salivary gland-specific probe to distinguish mutant from heterozygous embryos (arrowhead in I,J). Wild-type embryo genotypes are as follows: *rib*^{1}/CFL hybridized with *lacZ* (A) or stained with anti-βgal (E), Oregon R (C), and *rho*^{PΔ38}/TUL (G,G′,I).

at later stages, although they were often misrouted (data not shown). Migration of the other two primary branches (DB and VB) was generally unaffected, except for occasional extra DB cells (Fig. 2). The lumina of all branches of *rib* tracheae appeared more dilated than in wild type. It is possible that lumenal dilation is related to the early slowed outgrowth and stunting, either as a cause or effect. Alternatively, the two phenotypes could be independent. Both the lumen size and the migration defects in *rib* mutants are rescued by tissue-specific rescue with a *rib* transgene (Fig. 2K,L, see below), which demonstrates that *rib* function is required in tracheal cells.

rib and known signaling pathways in the trachea

To learn how *rib* functions with known signaling pathways to promote tracheal formation, we compared the tracheal defects in *rib* mutants with those in embryos in which the FGF, DPP, EGFR, or WG/WNT pathways were disrupted by following the expression of pathway-dependent tracheal markers. In the trachea, FGFR/BTL signaling is regulated by the spatially restricted expression of FGF/BNL (Fig. 1; Sutherland et al., 1996). To determine if *rib* defects were due to changes in *btl* or *bnl* expression, we examined RNA accumulation in *rib* mutants. Both *btl* and *bnl* RNA expression patterns were normal in *rib* mutants, except for a slightly prolonged expression of *btl* in the transverse connective (TC; Fig. 3A-D). Additionally, FGF-dependent MAPK activation at the tracheal pit stage (Gabay et al., 1997) was normal in *rib* mutants, as detected by staining with an antibody to the diphosphorylated, activated form of ERK (dpERK; data not shown). These findings reveal that *rib* does not function upstream of FGF signaling and that *rib* acts either downstream of or in parallel to FGF-dependent dpERK activation. *rib* mutants exhibited only a subset of defects observed in FGF signaling mutants; thus, if *rib* functions downstream of FGF signaling, it must do so in a spatially or temporally restricted manner.

DPP signaling is required for the DB, LT and GB, where it activates KNI expression which, at least in part, mediates the dorsoventral migration of these branches (Vincent et al., 1997; Chen et al., 1998). Since the incomplete migrations of the LT and GB in *rib* mutants could be caused by reduced DPP signaling, we asked whether *dpp* expression or KNI maintenance in the LT or GB was affected in *rib* mutants. *dpp* RNA was detected in the wild-type expression pattern, both dorsally and ventrally to the tracheal placode (data not

shown). As in wild-type embryos, KNI accumulation in *rib* mutants was detected in the early *rib* tracheal placode (data not shown) and was maintained in all branches of the trachea except the DT and TC, where it is normally lost (Fig. 3E,F). Thus, the stunted ventral branches in *rib* mutants are not caused by loss of KNI expression, and *rib* does not function upstream of DPP signaling. Moreover, if *rib* is required for DPP-dependent tracheal cell identity or migration, its requirement is limited to ventral cells (LT and GB) and is downstream of or parallel to activation of *kni* expression.

EGFR and WG/WNT signaling are both implicated in DT formation. Thus, *rib* could function with one or both of these pathways to promote DT migration. EGFR signaling was reported to specifically affect the formation of the DT and VB and to maintain expression of *sal* in the DT (Wappner et al., 1997). In embryos lacking EGFR signaling due to mutations in the receptor (*DER/faint little ball*), the ligand (*spitz*), or either of two upstream activators (*Star* and *rho*), many tracheal cells remain clustered near the tracheal pit (Wappner et al., 1997). Further analysis showed that not all placodal cells invaginate in *rho* mutants, leaving many cells on the surface of the embryo (Llimargas and Casanova 1999). Our analysis of *rho* mutants revealed that more DT cells and VB cells undergo normal primary branch migration than previously reported (Fig. 3G-J; Wappner et al., 1997). We also observed a significant loss of DB formation, and in most *rho* embryos, all branches contained fewer cells (Fig. 3G-H′). Moreover, we detected *sal* RNA expression in the dorsal region of the pits during stages 11-14 in *rho* mutants, although levels were not quite as high as in wild type (Fig. 3I,J). This result is in contrast to previous reports that *sal* is only expressed in the limited DT fragments that form between adjacent metameres in *rho* embryos (Wappner et al., 1997). Our findings support one of two models proposed by Llimargas and Cassanova (Llimargas and Cassanova, 1999) in which EGFR signaling is required for tracheal cell invagination, and defects in branch migration are an indirect consequence of having fewer cells at the appropriate position to receive and respond to spatial cues required for appropriate migration (such as WG signals to DT cells, see below). In contrast to defects caused by loss of EGFR signaling, mutations in *rib* affected DT migration more directly: all tracheal cells in *rib* mutants appeared to invaginate from the ectoderm, and DT cells were usually observed in a cluster at the TC below the DB cells. Additionally, expression of *rho*, which is involved in the spatial activation of EGFR, and EGFR-dependent dpERK were normal in *rib* mutants (data not shown), further indicating that *rib* acts independently of EGFR signaling.

Loss of WG/WNT signaling causes DT defects similar to those in *rib* mutants: the DT is absent and ‘pre-DT’ cells are clustered below the DB (Chihara and Hayashi, 2000; Llimargas, 2000). The only known early target of WG/WNT signaling in the trachea is the *sal* gene (Chihara and Hayashi, 2000; Llimargas, 2000), which is also required for proper DT migration (Kuhnlein and Schuh, 1996). In *rib* mutants, the spatial and temporal patterns of both *sal* RNA and SAL protein accumulation were unaffected, although levels appeared slightly reduced compared to those in wild-type embryos (Fig. 4A-D; data not shown). Since expression of *sal* in all tracheal cells (*btl-Gal4/UAS-sal)* did not increase DT cell migration (Fig. 4E,F), the slight reduction in *sal* expression

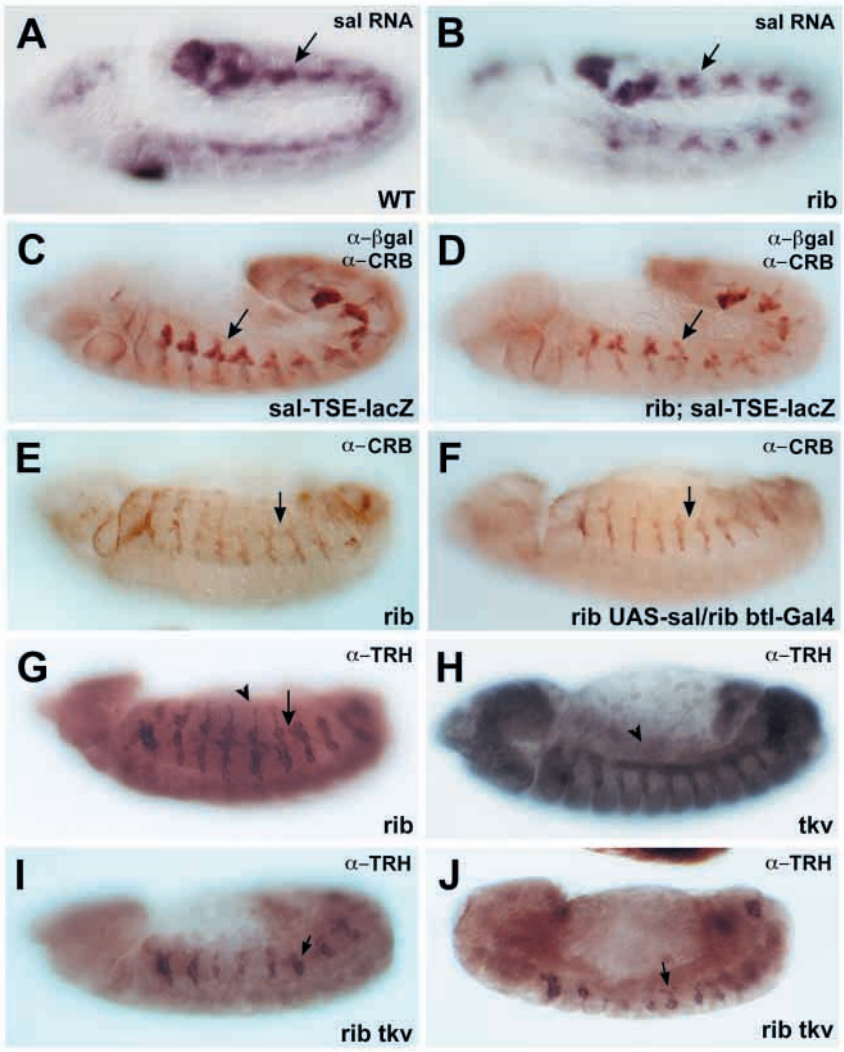

Fig. 4. *rib* functions downstream of, or in parallel to, WG signaling and is independent of *sal*. All views are lateral. Early stage 12 wild-type (A) and *rib*^{1} (B) embryos hybridized with an antisense *sal* RNA probe show *sal* accumulation in dorsal tracheal cells (arrow). Wild-type (C) and *rib*^{1} mutant (D) embryos carrying the *sal-TSE-lacZ* reporter construct stained with anti-β-gal, which detects expression in the dorsal tracheal cells (arrow), and with anti-CRB to visualize the trachea. Slightly lower levels of *sal*-β-gal are detected in *rib* mutants. Anti-CRB staining of a *rib*^{1} embryo carrying both *UAS-sal* and *btl-Gal4* transgenes (F) reveals that DT migration (arrow) is not rescued with increased *sal* expression compared with *rib*^{1} alone (E). The DT (arrow) in *rib*^{1} mutants fails to migrate (G), whereas the DB (arrowhead), LT, and GB fail to form in *tkv*^{A12} mutants (H). Embryos doubly mutant for *rib*^{1} and *tkv*^{A12} (I,J) form only the TC (arrow in I) and VB (arrow in J).

does not contribute to the *rib* phenotype. These experiments demonstrate that *rib* functions in DT cells downstream of or parallel to WG/WNT signaling and independently of *sal*.

In embryos doubly mutant for WG/WNT and DPP signaling, only VB cells migrate (Llimargas, 2000). Similarly, in embryos doubly mutant for *rib* and *thick veins* (*tkv*), which encodes one of the receptors essential for DPP signaling (Affolter et al., 1994), only VB cells migrated (Fig. 4G-J), a phenotype identical to that of embryos doubly mutant for *tkv* and *armadillo* (*arm*; Llimargas, 2000), which encodes an essential component of WG/WNT signaling (Peifer et al., 1993). Thus, like WG/WNT signaling, *rib* plays an instructive role in DT formation.

In *sal* mutants, DT cells migrate dorsally instead of forming the DT (Kuhnlein and Schuh, 1996), whereas in WG/WNT signaling mutants, DT cells are stalled at the TC. Thus, WG signaling must regulate other genes, in addition to *sal*, that control migration. Given that *rib* appears to phenocopy the loss of WG signaling in the DT, and that *rib* functions downstream of or in parallel to WG/WNT signaling, *rib* itself might be a target of WG/WNT signaling. *rib* RNA is expressed throughout the epidermis and is not obviously upregulated in the trachea (see below). Thus it is unlikely that *rib* is transcriptionally controlled by WG/WNT or other signaling pathways.

rib function in the epidermis

rib mutants fail to complete dorsal closure (Nüsslein-Volhard et al., 1984; Jack and Myette, 1997), the process by which the cells of the lateral epidermis move dorsally to encompass the amnioserosa and seal the dorsal surface of the embryo (reviewed by Noselli and Agnes, 1999). The Jun N-terminal kinase (JNK) signaling pathway (reviewed by Noselli and Agnes 1999) and the WG signaling pathway (McEwen et al., 2000) are required for dorsal closure. Both pathways are necessary for the characteristic cell shape changes in the leading edge cells and the transcriptional activation of *dpp*. As reported by Blake et al., *rib* mutants also lack the characteristic elongation of the cells at the leading edge, and at late stages, these cells are large and misshapen (Blake et al., 1998).

To determine whether the dorsal closure defects in *rib* mutants are related to defects in JNK or WG signaling, we analyzed the dorsal cuticle of larvae carrying different allelic combinations of *rib* mutations. In the allelic combinations that could be scored (i.e., those in which sufficient cuticle was produced), approximately two-thirds of the larvae had a large dorsal hole, and one-third had a small anterior dorsal hole with a puckering of the remaining dorsal cuticle (Fig. 5A-C). This range of phenotypes is similar to the defects in larvae with loss-of-function mutations in either JNK or WG pathway components. We also investigated whether *dpp* expression was maintained in the leading edge cells of *rib* mutants. Unlike mutations in either JNK or WG signaling components, in which *dpp* expression is absent in leading edge cells *dpp* expression was observed at high levels in the leading edge cells in *rib* mutants (Fig. 5D,E). At late stages, *dpp* expression was often observed in lateral patches. This apparent increase of *dpp* expression in *rib* mutants could be due to increased numbers of cells expressing *dpp*, increased size of leading edge cells and/or loss of cell cohesion (which could cause cells to

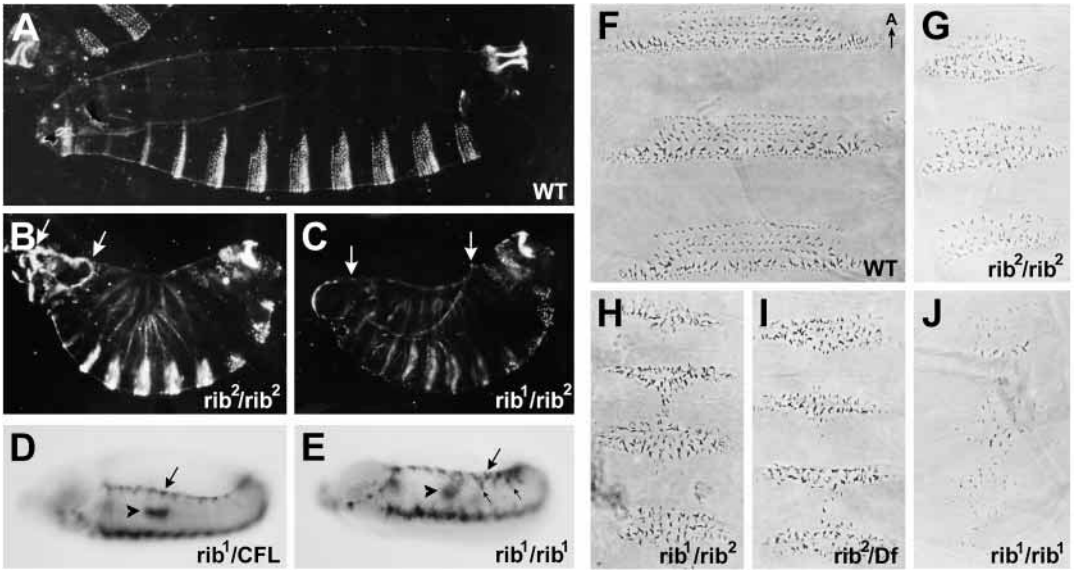

Fig. 5. *rib* mutants fail to complete dorsal closure and have ventral cuticle patterning defects. Dark-field images of the lateral cuticle of wild type (A) and *rib* mutant larvae (B,C) photographed at the same magnification. Of the mutant larvae with scorable cuticles, small anterior dorsal holes and puckering of the dorsal epidermis occur in 36% of *rib* mutants (B) and large dorsal holes occur in 64% of *rib* mutants (C; arrows indicate extent of dorsal opening). Lateral views of *dpp* RNA expression in the leading edge cells of the lateral epidermis (large arrow) and the midgut (arrowhead) of *rib*/CFL (D) and *rib* mutant (E) embryos are shown. In *rib* mutants, *dpp* staining at the leading edge is more disorganized and in some regions extends into the lateral epidermis (small arrows in E). This apparent increase may be due to an increase in the number of cells expressing *dpp* or the morphology of these cells and the leading edge at late stages. (F-J) Representative phase contrast images of ventral cuticles of first instar larvae of an allelic series of *rib* mutations. Anterior (A) is oriented up, and larvae were photographed at the same magnification. There is a prominent narrowing of the lateral extent of denticle belts relative to the ventral surface of the larva, increasing with allele severity. Loss of denticle diversity also increases with the allelic series. The most severe phenotype (rib^1/rib^1) is shown in J and is equivalent to $rib^1/Df(2R)P34$ (not shown); in such embryos, only a few similarly shaped denticles form.

collapse or remain in more ventral positions). In any case, this experiment reveals that, as in the trachea, *rib* is not an upstream activator of JNK or WG signaling and that JNK- and WG-dependent activation of *dpp* is not mediated by *rib*. Mutations in *rib* caused defects at an earlier step in dorsal closure than *dpp* mutations: the leading edge cells fail to change shape in *rib* mutants, whereas DPP signaling is required for cell shape changes and movement of the ectodermal cells just ventral to those at the leading edge (Riesgo-Escovar and Hafen, 1997). Thus, if *rib* functions downstream of the JNK or WG pathway to mediate dorsal closure, it must be acting in parallel to *dpp* activation.

Patterning in the ventral cuticle is also impaired in *rib* larvae, which exhibit both a narrowing of the lateral extent of denticle belts and a fusion of belts at the midline (Fig. 5F-J; Nüsslein-Volhard et al., 1984). At a gross level, these phenotypes are similar to those described for the EGFR signaling mutants, *rho* and *spitz* (Raz and Shilo, 1993). We examined the cuticle phenotypes of different allelic combinations of *rib* mutations, scoring both the lateral extent of denticle belts and denticle diversity. The lateral extent of *rib* denticle belts was narrowed to 37%, 46% and 70-100% of the wild-type width, consistent with an allelic series ($rib^2/rib^2 < rib^2/rib^1 = rib^2/Df < rib^1/rib^1 = rib^1/Df$; Fig. 5F-J). rib^1/rib^1 and rib^1/Df cuticles were often very hard to detect, suggesting that very little cuticle is secreted.

The loss of denticle diversity in *rib* mutants also corresponded to the above allelic series. The least affected cuticles had the most diversity of denticle types (rib^2/rib^2; Fig. 5G), whereas more severely affected cuticles had only one or two denticle types (rib^2/rib^1 and rib^2/Df; Fig. 5H,I), and the most severely affected cuticles had very few faint denticles which appeared to be of a single type (rib^1/rib^1 and rib^1/Df; Fig. 5J). The denticle belts of *rib* larvae with a single denticle type looked notably similar to larvae simultaneously lacking the late activities of WG and EGFR signaling, in which all denticles are type 5 (wg^{ts}, *UAS-DN-DER*, *arm.Gal4*; Szuts et al., 1997). Unlike WG/EGFR-deficient larvae, however, not all of the denticles in *rib* mutants were oriented posteriorly. Overall, the dorsal and ventral cuticle phenotypes, together with the tracheal defects, suggest that *rib* may function with a combination of signaling pathways. It is clear that *rib* does not function upstream of these pathways, nor does *rib* interfere with transcriptional activation of early target genes. Thus, *rib* functions downstream of or parallel to these pathways to promote cellular changes.

Directed migration of the salivary gland is defective in *rib* mutants

Signaling pathways controlling cell migration in the embryonic salivary gland have not yet been identified. Nonetheless, the salivary gland, like the tracheal system, invaginates through a stereotypical process involving directed cell migration (Fig. 6; reviewed by Myat et al., 2000) The salivary glands form from two paired primordia that arise from the ventral ectoderm of parasegment two. Through changes in cell shape and migration, the primordia are internalized and ultimately give rise to two cell types: secretory and duct. The secretory cells are the first to invaginate and proceed in an ordered, sequential manner beginning with the cells in the dorsal posterior region of the primordium (Myat and Andrew, 2000). The secretory cells move dorsally into the embryo, then turn and migrate posteriorly until the distal half of the gland reaches the level of the third thoracic segment. After the movements of head involution, the salivary glands lie closer to the anterior end of the embryo and are oriented along the anteroposterior axis. Concomitant with later secretory cell migrations, the duct cells undergo a complex set of morphogenetic movements to create a tubular structure. This tube starts at the larval mouth and then branches to connect to the two secretory glands (Fig. 6K; Kuo et al., 1996).

Although salivary glands were reported to be abnormal in late stage *rib* mutant embryos, earlier stages were not analyzed (Jack and Myette, 1997). As with the tracheal primordia, the secretory gland primordia in *rib* mutants were indistinguishable from those in wild-type embryos, and the initial invagination proceeded normally (Fig. 6A,B); however, *rib* secretory cells did not migrate past the point at which wild-type cells turn and migrate posteriorly (Fig. 6C-F). Thus, the secretory cells in *rib* mutants never reach their final destination. At late stages, the lumina of the salivary glands were greatly enlarged compared to wild-type glands (Fig. 6G,H), suggesting that *rib* may also play a role in maintaining organ shape once the salivary gland has formed. Expressing a *rib* transgene specifically in the secretory cells of *rib* mutants (see below) restored both directed migration and lumen size (Fig. 2I,J). Thus, *rib* function is required in secretory cells to control migration and organ shape.

The salivary duct also failed to undergo proper morphogenesis in *rib* mutants. Two duct markers, TRH protein and *btl* RNA, were detected in a normal pattern in the duct primordia of *rib* mutants (data not shown). In contrast, duct cells stained poorly for the Dead ringer (DRI) protein, which is normally expressed robustly by stage 13; only diffuse low levels of DRI expression were detected in *rib* mutants prior to stage 15. In late stage *rib* mutant embryos, we observed either no tubes or rudimentary individual tubes connected to the secretory glands; these semi-tubular structures did not elongate and never elaborated into a normal duct (Fig. 6L,M). In embryos expressing a *rib* transgene in secretory cells of *rib* mutants (see below), duct formation was restored (Fig. 6N). This result indicates that *rib* duct defects are indirect and suggests that duct formation requires proper secretory cell morphogenesis. While both salivary gland structures are abnormally formed in *rib* mutants, there is a specific requirement for *rib* in the secretory cells for their posterior migration, similar to the requirement for *rib* in the tracheal DT cells for their anteroposterior migration.

Identifying the *rib* transcripts

Our phenotypic analysis suggested that *rib* may respond to signals by activating changes required for directed cell movements during organogenesis. To understand the molecular mechanism by which *rib* functions, it was essential to identify and characterize the *rib* gene. *rib* maps to 2-88 (Tearle and Nüsslein-Volhard, 1987) and is uncovered by *Df(2R)P34* (Blake et al., 1998). Complementation analysis with overlapping deficiencies revealed that *rib* function was also removed by *Df(2R)GC8*, but not by *Df(2R)GC10*, *Df(2R)F7*, or $EP(2)2445^{\Delta 1}$, a small deficiency we generated using a nearby P element (Fig. 7; Table 3). Thus, *rib* maps distal to $EP(2)2445^{\Delta 1}$ and proximal to or spanning the distal breakpoint

of *Df(2R)P34*. By mapping deficiency breakpoints in combination with sequence information from the Berkeley Drosophila Genome Project (BDGP) and Celera Genomics (Adams et al., 2000), we identified three genes in this interval: *windbeutel* (*wbl*) and two uncharacterized genes (Fig. 7B). Mutations in *wbl* complemented rib^1 (Table 3), and a genomic wbl^+ transgene (Konsolaki and Schupbach, 1998) did not rescue *rib* lethality in any allelic combination (data not shown). Based on the complementation data and on the observation that *wbl* mutants did not exhibit embryonic defects similar to *rib* (data not shown), we conclude that *rib* is not allelic *wbl*.

We examined the RNA expression patterns of the two remaining genes that map to the *rib* interval (genes *4* and *5*). Gene *4* was not detectably expressed in wild-type embryos as assayed by whole-mount in situ hybridization and northern analysis (data not shown). Since *rib* function is required during embryogenesis, gene *4* is not likely to encode RIB. The remaining candidate, gene *5*, was expressed in a complex and dynamic pattern in nearly all tissues during embryonic development, with higher levels in several tissues affected by *rib* mutations including salivary gland, epidermis, and Malpighian tubules (Fig. 8). We also detected nucleotide (nt) changes in the corresponding open reading frame (ORF) in both *rib* alleles (see below). Finally, by expressing gene *5* ORF in the tracheal system and salivary gland, we detected tissue-specific rescue of tracheal branch migration (Fig. 2K,L) and salivary gland posterior migration (Fig. 6I,J). This experiment conclusively demonstrated that gene *5* encodes RIB and that RIB function is required in tracheal and salivary gland secretory cells to control migration.

rib encodes a novel BTB/POZ protein

rib encodes a 1983 nt ORF corresponding to a 661-residue protein with an amino- (N) terminal BTB/POZ (Bric a brac, Tramtrack, Broad-Complex/Poxvirus, zinc finger) domain (Fig. 9). The BTB/POZ domain is an evolutionarily conserved

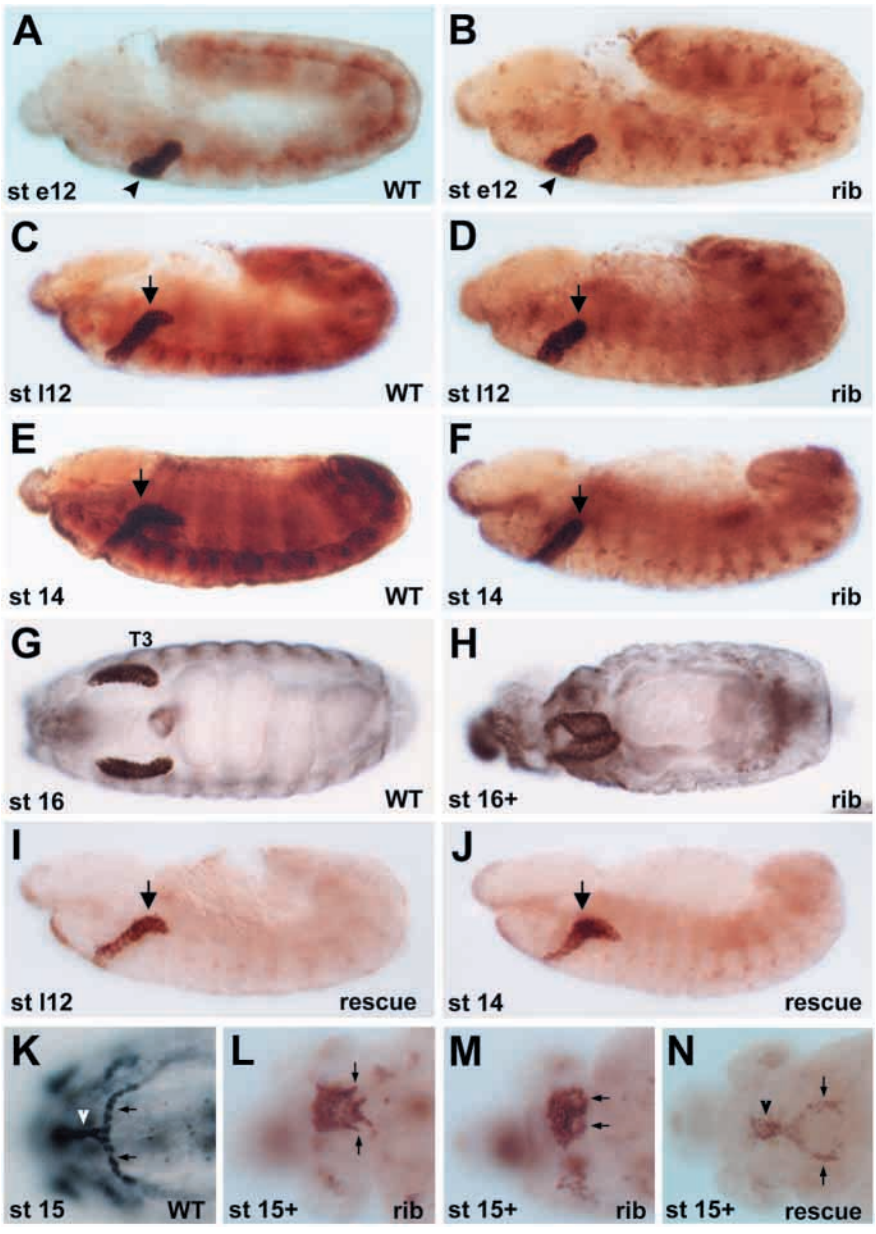

Fig. 6. *rib* mutants have defects in salivary gland formation. (A-J) Salivary gland secretory cells (arrowheads in A,B) are visualized with an antibody to dCREB-A. (K-N) Salivary duct cells are visualized with an antibody to DRI. A-F, I, and J are lateral views; G,H,K-N are ventral views. In the formation of the wild-type salivary gland, cells are internalized (A), migrating first dorsally and then redirecting to migrate posteriorly (arrow in C,E) until the dorsal tip reaches the level of the third thoracic segment (T3), and the glands lie along the body wall (G). Initially, rib^1 secretory cells invaginate similarly to wild-type (compare B and A); however, once cells reach the dorsal position at which wild-type cells would normally turn to migrate posteriorly, rib^1 secretory cells are stalled in their migration (arrow in D,F). In late stage *rib* mutants, the salivary glands become reoriented, which is likely a secondary effect, and the lumina of the gland become greatly distorted (H). In embryos carrying *UAS-rib* and the secretory cell-specific driver *fkh-Gal4*, the posterior migration of secretory cells is restored (I), and secretory cells reach their normal position in the embryo (J). Wild-type salivary ducts are composed of two individual ducts (arrows in K) and a single common duct (arrowhead in K). Salivary ducts in *rib* mutants fail to complete normal development. Images representing the range of duct defects are shown (L,M). In some embryos, one or two rudimentary tubes are formed, most likely corresponding to the individual ducts (arrows in L), but these never elaborate. In other embryos, no tubes form and the anterior portion of the secretory gland is found in a hole in the DRI-stained duct primordia (arrows in M). In embryos carrying *UAS-rib* and the secretory cell-specific driver *fkh-Gal4*, formation of both the common (arrowhead in N) and individual ducts (arrows in N) is significantly restored. Wild-type embryos are rib^1/CFL co-stained with anti-βgal (brown staining in A,C,E) or *Oregon R* (G,K).

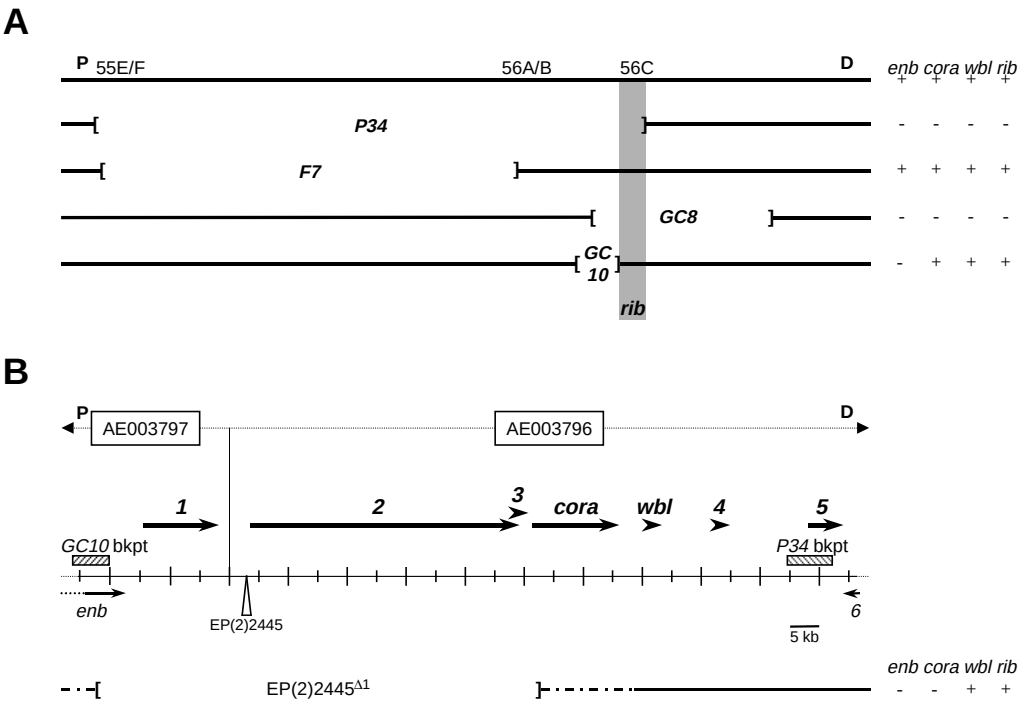

Fig. 7. Genomic region surrounding *rib*. (A) *rib* maps to a small interval of the 56C region (gray) by complementation analysis with overlapping deficiencies in the region (*Df(2R)P34*, *Df(2R)F7*, *Df(2R)GC8*, and *Df(2R)GC10*). *coracle* (*cora*) and *wbl* also map within the *rib* region, whereas *enabled* (*enb*) maps to a distinct interval (Gertler et al., 1995). (B) Two Celera Genomics DNA contigs span the *rib* region. AE003796 begins distal to the region, ending at nt 268,419, which overlaps with the first 60 nt of AE003797; AE003797 continues proximally, ending outside of the region. Breakpoints for *Df(2R)GC10* and *Df(2R)P34* are shown as hatched boxes. *1*, *2*, *3*, *4*, *5* and *6* are predicted genes in the region. Genes are depicted as arrows, which indicate the direction and approximate size of the transcription unit. *gene 6* maps completely outside of deficiency *Df(2R)P34*. *EP(2)2445* is the viable P-element insertion line used to generate the lethal line *EP(2)2445*$^{\Delta 1}$, which deletes DNA from *enb* to *cora* and does not affect *rib* function, leaving only three candidates. Since *wbl* complements *rib* (Table 1), *rib* is gene *4* or gene *5*. Proximal (P) and distal (D) is relative to the centromere.

domain that mediates homo- or heterodimerization with other BTB/POZ domains (Bardwell and Treisman, 1994; Chen et al., 1995) and is found in over 400 proteins. A short coiled-coil region in the carboxy (C) terminus is predicted. RIB has four consensus nuclear localization signals (NLS), two of which are bipartite, and RIB is predicted to be nuclear by the PSORT program. Thus, RIB may function in the nucleus. RIB also contains consensus phosphorylation sites for a number of kinases that mediate the formation of tissues in which *rib* is required (e.g., MAPK). Consensus glycosylation, myristylation and amidation sites are also present in the *rib* ORF.

In the more severe allele *rib*^{1}, we detected a single nucleotide change in the *rib* ORF that results in a nonsense codon after residue 282 (Fig. 9B). This mutation deletes the entire C-terminal half of the protein, and is likely to be null, consistent with phenotypic analysis. *rib*^{2} has a single base change that replaces arginine 58 with a histidine (R58H) in the BTB/POZ domain. A mutation in *rib* was also discovered on the *zipper*^{1} (*zip*^{1}) chromosome (Blake et al., 1998). We confirmed that *zip*^{1} mutants fail to complement both *rib* alleles, sequenced the *rib* ORF on the *zip*^{1} chromosome, and found the identical nucleotide change that created the R58H mutation in *rib*^{2}. This result is consistent with the phenotypic report that, when recombined off the *zip*^{1} chromosome, the *rib*^{z1} allele behaves like *rib*^{2} and is not as severe as *rib*^{1} (Blake et al., 1998). It is not clear whether the *zip*^{1} chromosome recombined with *rib*^{2} at some point, or whether finding the identical residue substitution indicates the importance of R58 in RIB function. All other detected base changes that resulted in residue substitutions were detected on all *rib* chromosomes and/or on the balancer chromosome, suggesting that these other changes are polymorphisms not responsible for *rib* phenotypes.

Table 3. Complementation analysis of *rib* and local deficiencies or mutants

	rib^{1}	*rib*^{2}	*EP(2)2445*$^{\Delta 1}$
Df(2R)P34	225:0	204:0	164:0
Df(2R)F7	40:28	106:53	138:45
Df(2R)GC8	79:0	134:0	197:0
Df(2R)GC10	54:35	159:98	191:7
EP(2)2445$^{\Delta 1}$	121:60	51:28	102:0
EP(2)2445$^{\Delta 2}$	115:73	54:33	67:0
cora^{4}	65:36	95:50	211:0
wbl^{M46}	226:102	364:4	72:39
wbl^{M88}	230:98	64:2	81:36
wbl^{E4}	145:100	250:17	–
wbl^{RP}	247:117	204:39	–
wbl^{T6}	–	122:32	–

Numbers represent balancer (CyO):non-balancer (non-CyO) flies counted. *EP(2)2445*$^{\Delta 1}$ and *EP(2)2445*$^{\Delta 2}$ are excision alleles generated from the viable *EP(2)2445* line. *wbl* showed reduced viability in *trans* to *rib*^{2}, a phenotype ameliorated by the *wbl*$^{+}$ rescue transgene (data not shown). Sequence analysis of the *rib*^{2} chromosome revealed a base change in *wbl* that substitutes a glutamate for glycine at residue 87 (G87E). Since G87 is conserved in homologous proteins (Konsolaki and Schupbach, 1998), the G87E mutation could explain the *wbl*/*rib*^{2} genetic interaction.

DISCUSSION

rib is required for the formation of several embryonic tissues. In *rib* mutants, both tracheal cells and salivary gland secretory cells fail to complete characteristic migrations along the anteroposterior axis, indicating that *rib* is required for directed cell movements. Late in embryogenesis, once organs have

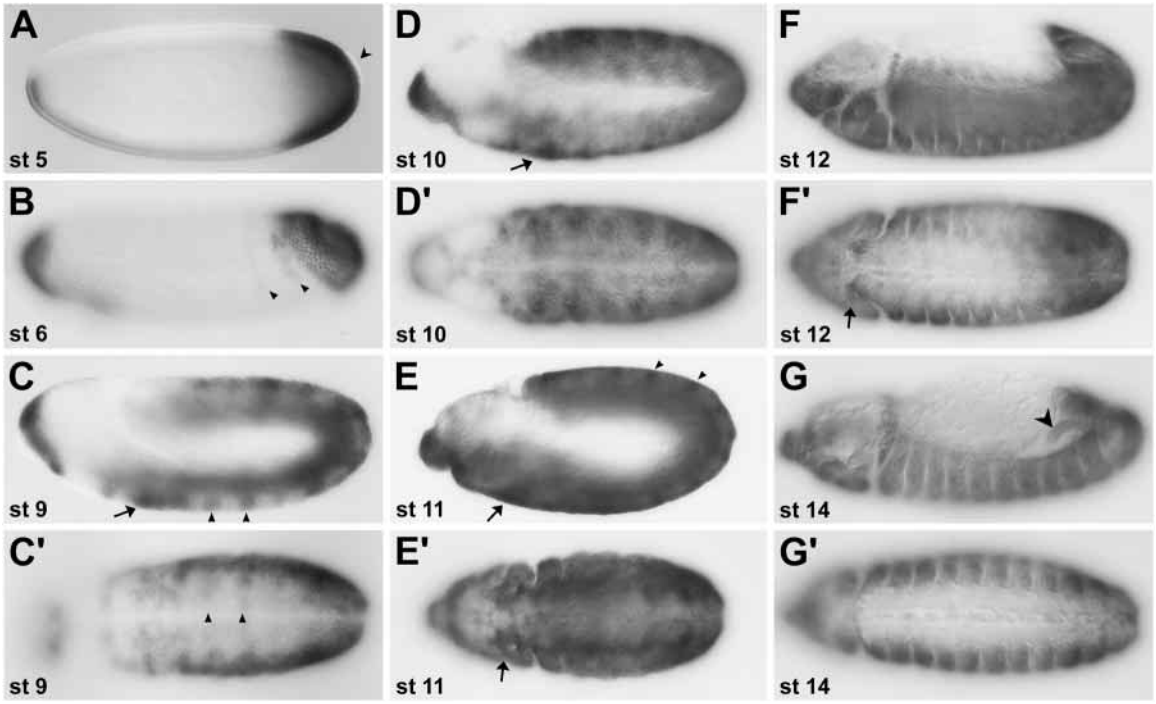

Fig. 8. *rib* mRNA is expressed throughout embryonic development. Whole-mount in situ hybridization to wild-type embryos with an antisense *rib* RNA probe. Images with primed letters are ventral views of the same embryo; all others are lateral views. Embryonic stages are indicated in the lower left corner. *rib* expression is first detected in the termini (A,B), but is absent from pole cells (arrowhead in A). Segmental stripes appear in the epidermis (arrowheads in B,C,C′,E). Expression of *rib* RNA in the salivary gland primordia is evident by stage 10 (arrow in D), and is expressed throughout invagination (arrows in E,E′,F′). The Malpighian tubules also express *rib* (arrowhead in G). By later stages, *rib* RNA is detected in most cells of the epidermis, including cells of the lateral epidermis. Of note is the lack of elevated expression in the later central nervous system and midgut, two tissues whose formation is abnormal in *rib* mutants (Jack and Myette, 1997), perhaps indicating that these defects are indirect. Alternatively, earlier expression or a lower level of *rib* is required in these tissues.

formed, the salivary gland lumen becomes abnormally dilated, suggesting a role for *rib* in cell shape maintenance. In tracheal development, *rib* may function with WG/WNT and/or FGF signaling to direct the migration of the cells that give rise to the dorsal trunk. Incomplete dorsal closure and defective ventral cuticle patterning in *rib* mutants are also consistent with an interaction of *rib* with WG and/or MAPK signaling. Our phenotypic analysis of *rib* suggests that directed cell movements are regulated by the same components used in cell shape maintenance. Lastly, we show that the *rib* gene is expressed widely throughout development and encodes a novel protein with a BTB/POZ domain.

rho, *rib* and tracheal branch formation

We have made two observations that support a model proposing that the primary role for EGFR signaling is the invagination of tracheal primordia and that defects in branch migration may be an indirect result of reduced invagination (Llimargas and Casanova, 1999). (1) All branches contained fewer cells in *rho* mutants, hence no particular branch identity is lost. (2) *sal* expression in the dorsal tracheal cells of *rho* mutants during primary branch outgrowth is normal, suggesting that EGFR is not required to specify cell fate within the placode (at least as measured by expression of this DT-specific gene). Thus, EGFR signaling may only regulate invagination, which would position cells to receive subsequent signals specifying branch fate.

Analysis of WG signaling in tracheal branching (Chihara and Hayashi, 2000; Llimargas, 2000) suggests that cells are allocated to branches (cell allocation) independently from cell fate specification. (1) In WG signaling mutants the ‘pre-DT’ cells are positioned correctly, but fail to migrate away from the TC. (2) WG signaling mutants do not express *sal*, a DT-specific marker. Thus, the cells are allocated to the DT, but do not express DT markers or behave like DT cells. *rib* mutants, like WG/WNT signaling mutants, also failed to form the DT, and ‘pre-DT’ cells were stalled at the TC; however, unlike embryos lacking WG signaling, *rib* mutants expressed *sal* in DT cells. Thus, *rib* is not required for cell allocation or cell fate specification (as monitored by *sal*), but is only required for branch migration. In summary, these observations suggest that, at least for the tracheal DT, cell allocation is independent of cell fate specification, and cell fate can be further subdivided into branch identity (controlled by genes such as *sal* that specify branch features; Chen et al., 1998) and branch migration, which involves *rib*. We are currently limited by the number of markers available to assess specific tracheal cell fates and the independence of these processes. The identification of new branch-specific markers and mutations will allow us to further refine models for tracheal branching.

rib may function with multiple signaling pathways

The similarity of the tracheal DT phenotypes in *rib* mutants and WG signaling mutants raises the possibility that *rib*

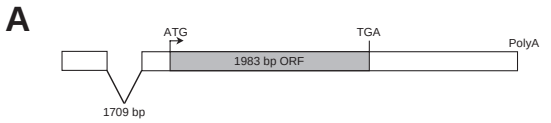

B

MGGPTAPVASSGEVG**QTYCLRWNNHQTNLVQILHALHEVGSYVDCSLVVD**

DEQFQAHR(rib²: H)**VVLAANSPYFQHILKDVPQDHCSIILPGVKGFEIAALLQYMY**

TGETTVTKSQEPEILRTAKELQVKGLYDNLMKFNHASVTPTSSSGAGGAK

PQNGSASNHSSSVISTSTHISPSAAISSSCSPPPPPQFGYQPGYSHYPQQ

QPMSASQIPAGEAPLTPTQATPHSAASGAGEAGGQWPLTPSAAAAMLNSV

YESAADMNPLKRKKLSAISSMLLSGNRDTPIL(rib¹ STOP)RNVLAQANPADSSQPGPM

NANGEKTPTHPHQNTQLPAGLGVSGGERNHSFNGSDYGGDKEPLSPYTDR

SFEEETGQSGGKKPEWKRYKQYTRADMMCAIQAVREGMSALQASRKYGLP

SRTLYDKVRKLNITTGRGTHRTPKRSPPGAESSQGFSYSAAAAAAAHNYG

HGHGHHSEVKRDQKVDHVPAHHGMPPTIPPSAAALLDHAFLQQALENRGG

DMAGREALHAMALAAAAHAAANRLSSSPAEMDQRSNGHGMRSPSPQGRHY

PHEQEAMDLEMEKHEQNIIKRERDQDEREDADDEEDHEQEHVEDLSLARK

ERPPSPYSPQPTEAGAGVIMHASSASANGKDHVDY PSSPQFVPIGLKREL

MEGEDAQARAD

Fig. 9. (A) Gene structure of *rib*. The salient features of the longest cDNA (3959 nt; BDGP LD16058) are depicted, and the position of the single intron is noted. A consensus polyadenylation signal (AATAAA) is present near the end of the 3′ UTR. By northern analysis, we detected a single transcript of 4.3 kb (data not shown), which correlates well with cDNA length and suggests the cDNA is nearly full length. (B) Conceptual translation of the 1963 nt ORF yields a 661-residue protein. Translation of the corresponding GadFly gene CG7230 reveals an identical protein sequence. An N-terminal BTB/POZ domain is denoted in bold. There are four consensus NLSs (underlined). A predicted coiled-coil region in the C terminus is double underlined. RIB contains seven MAPK consensus phosphorylation sites ($PX_{1\text{-}2}S/TP$, where X is any amino acid), which are boxed. The mutations in *rib*^{1} and *rib*^{2} alleles are double-boxed: *rib*^{1} encodes a stop codon after residue 282, and *rib*^{2} has an arginine to histidine substitution at residue 58 (R58H). (C) Sequence alignment of the RIB BTB/POZ domain with BTB/POZ domains of *Drosophila* Longitudinals lacking (LOLA), *Drosophila* Bric a brac (BAB), mouse Zinc finger protein 161 (mZfp161), and human Promyelocytic leukemia zinc finger (hPLZF). The eleven N-terminal residues (under the bar) are not included in the BTB/POZ domain as defined by the InterPro program; however, this short stretch is highly conserved in these three and other *Drosophila* BTB/POZ domain proteins. Percentage identity and similarity of the BTB/POZ domains with respect to RIB are noted. Residues that were examined in a structure/function analysis of hPLZF (Melnick et al., 2000) are indicated by an open circle, and residues that, when mutated, disrupt BTB/POZ domain function are also indicated by a filled circle. Note that the *rib*^{2} allele has a change in one of these essential residues (*). Black shading, white letters denotes identical residues; dark gray shading, white letters denotes conserved residues; grey shading denotes similar residues.

C

```
RIB      16:QTYCLRWNNHQTNLVQILHALHEVGSYVDCSLVVDDEQFQAHRVVLAANSPYFQHILKDVPQDHCSIILP
LOLA      5:QQFCLRWNNHQSTLISVFDTLLENETLVDCTLAAEGKFLKAHKVVLSACSPYFATLLQEQYDKHPIFILK
BAB     100:QQFCLRWNNYQTNLTTIFDQLLQNECFVDVTLACDGRSMKAHKMVLSACSPYFQTLLAETPCQHPIVIMR
mZfp161   9:ETIKYNDDDHKTLFLKTLNEQRLEGEFCDIAIVVEDVKFRAHRCVLAACSTYFKKLFKKLEVDSSSVIEI
hPLZF     7:GMIQLQNPSHPTGLLCKANQMRLAGTLCDVVIMVDSQEFHAHRTVLACTSKMFEILFHRNSQHYT....L
```

```
RIB      86:GVKGFEI.AALLQYMYTGETTVTKSQEPEILRTAKELQVKGLYDNLMKFNHASV
LOLA     75:DVKYQEL.RAMMDYMYRGEVNISQDQLAALLKAAESLQIKGLSDNRTGGGVAPK
BAB     170:DVNWSDL.KAIVEFMYRGEVSVSQDQIGPLLRIAEMLKVRGLADVTHMEAATRA
mZfp161  79:DFLRSDIFEEVLNYMYTAKISVKKEDVNLMMSSGQILGIRFLDKLCSQKRDVSS
hPLZF    73:DFLSPKTFQQILEYAYTATLQAKAEDLDDLLYAAEILEIEYLEEQCLKMLETIQ
```

%ID	%SIM
41	60
38	59
28	51
25	43

functions with WG signaling for migration of DT cells. *sal* is the only known early downstream target of WG/WNT signaling in the DT. Because the DT phenotype is more severe in embryos lacking WG/WNT signaling than in *sal* mutants, there must be additional downstream targets of WG signaling. Indeed, we can predict that these other genes control migration based on two findings. (1) DT cells are capable of migrating in *sal* mutants, but move in the wrong direction (dorsally; Kuhnlein and Schuh, 1996). (2) When both WG and DPP signaling are activated in wild-type embryos (activated *arm* and activated *tkv* in all tracheal cells), a complete longitudinal DT forms that does not express *sal* (Llimargas, 2000), suggesting that *sal* may be dispensable for anteroposterior migration in some cases. We have shown that loss of *rib* results in a DT phenotype identical to that observed in loss of WG/WNT signaling and that *rib* functions in parallel to WG/WNT-dependent *sal* expression. Together these results suggest that *rib* is working with WG/WNT signaling, either in parallel or potentially as a downstream target, to direct DT migration.

We hypothesize that *rib* may respond to signals from multiple pathways based on our analysis of the ventral cuticle phenotype. In *rib* mutants, the defects in ventral cuticle patterning appeared most similar to the phenotype reported for the combined loss of late WG signaling and EGFR signaling (Fig. 5; Szuts et al., 1997). In this tissue, *rib* could be integrating signaling from WG and EGFR. In several other tissues requiring *rib* function, WG signaling and signaling through a MAPK cascade are also required; however, in these cases, loss of either of the individual pathways results in phenotypes similar to those of *rib* mutants. For instance, *rib* is required for the cell shape changes in the leading edge cells during dorsal closure (Blake et al., 1998), a process that requires both WG signaling (reviewed by Noselli and Agnes 1999) and JNK signaling (McEwen et al., 2000). The second midgut constriction and the morphogenesis of the Malpighian

tubules are defective in *rib* mutants (Jack and Myette, 1997), and both events also require both WG and EGFR signaling (reviewed by Bienz 1994; Skaer and Martinez Arias, 1992; Baumann and Skaer, 1993; Kerber et al., 1998; Szuts et al., 1998; Wan et al., 2000). Similarly, in the trachea, *rib* could respond to WG signaling and either of the two pathways (FGF or EGFR) that activate the MAPK cascade in tracheal cells. Since the *rib* phenotype is distinct from EGFR signaling mutants, we favor a role for *rib* downstream of FGF signaling. Indeed, the stalled outgrowth of all tracheal branches and stunted ventral branches observed in *rib* mutants may be linked to FGF signaling. Consistent with the idea that *rib* responds to MAPK signaling, the RIB protein has seven consensus MAPK phosphorylation sites.

rib may direct cell movements by regulating the cytoskeleton

rib is thought to be required for generating specialized cell shapes. For instance, during dorsal closure, leading edge cells of the lateral epidermis fail to elongate in *rib* mutants (Blake et al., 1998). *rib* mutants also show abnormal dilation of salivary gland lumina in late embryogenesis (this work; Jack and Myette, 1997), suggesting that either *rib* is also required at late stages to maintain organ shape or loss of early *rib* function indirectly causes the late lumenal dilation. *rib* appears to control cell shapes by regulating the cytoskeleton. During dorsal closure, a band of actin and myosin forms at the dorsal margin of leading edge cells (Young et al., 1993). In *rib* embryos, the actin band is narrower and myosin heavy chain (MHC) is absent from leading edge cells (Blake et al., 1998). Thus, *rib* may be required for the localization or organization of cytoskeletal components. *zip* encodes a nonmuscle MHC and is required in many of the same tissues as *rib*; however, strong loss-of-function mutations in *zip* suppress the distended lumenal phenotype of *rib* salivary glands, suggesting that *rib* does not positively regulate myosin activities (Blake et al., 1999). Instead, *rib* may repress myosin contraction or regulate the direction of contraction, perhaps by providing a balancing force to the direction of basal myosin contractions. Our studies reveal a role for *rib* in coordinating directed cell migration, a process that clearly involves actin/myosin dynamics. Thus, *rib* may modulate actin/myosin behavior for cell movement and cell shape during both tissue formation and tissue homeostasis. If *rib* is responding to signaling pathways, *rib* could be a critical factor linking signaling events to changes in the cytoskeleton.

The *rib* gene encodes a novel protein with two protein-protein interaction domains, an N-terminal BTB/POZ domain and a C-terminal coiled-coil region. The BTB/POZ domain mediates dimerization (Bardwell and Treisman, 1994; Chen et al., 1995), and BTB/POZ proteins often contain additional domains that define protein function and/or subcellular localization. Many BTB/POZ proteins contain multiple DNA binding zinc fingers and function as transcriptional regulators. For example, the *Drosophila* Tramtrack protein is required to represses transcription of pair-rule genes in early embryogenesis (Harrison and Travers, 1990). BTB/POZ domain proteins can also mediate cytoskeletal organization. For instance, the *Drosophila* Kelch protein, which oligomerizes via its BTB domain and binds actin through its kelch domains, is required to maintain cytoskeletal organization of ring canals during oogenesis (Robinson and Cooley, 1997). BTB/POZ proteins can also function outside the cell; the mammalian BTB/POZ protein Mac-2 binding protein (M2BP) localizes to the extracellular matrix (ECM) and forms multivalent ring structures proposed to be important for its interactions with collagens IV, V and VI, fibronectin, and other ECM proteins (Müller et al., 1999). One family of *Arabidopsis* BTB/POZ-containing proteins has a composition very similar to that of RIB: a BTB/POZ domain at the N-terminus and a coiled-coil at the C terminus (Sakai et al., 2000). One family member, RPT2, appears to respond to signals that promote phototropism. RPT2 also contains an NLS; however, it is not yet known where RPT2 functions. Based on the four putative NLSs, we speculate that RIB may function in the nucleus, where it would be positioned to regulate the expression of genes required for cytoskeletal changes during morphogenesis. Alternatively, RIB may reside in the cytoplasm and more directly regulate cytoskeletal organization. Since BTB/POZ domains can heterodimerize, RIB may have a partner(s) providing additional functional motifs. *rib* RNA is expressed in a dynamic pattern during development, including expression in cells that appear phenotypically normal in *rib* embryos. Thus, *rib* function is likely to be post-transcriptionally regulated, perhaps through the phosphorylation of its MAPK sites or through limited expression or activation of cofactors. Further investigation of *rib* may help us to better understand the mechanisms by which cells control the direction of migration during development.

We are grateful to A. Haberman, D. Montell, M. M. Myat, K. Wilson, and an anonymous reviewer for helpful comments on the manuscript. We thank the Bloomington and UMEA Stock Centers, M. Affolter, R. Fehon, S. Hayashi, T. Laverty, R. Schuh, T. Schüpach, and B. Shilo for providing fly strains. We also thank W. Gelbart, S. Hayashi, M. Konsolaki, and D. Montell for providing DNAs and A. Haberman, P. Israel-Johnson, E. Knust, D. Kosman, M. Petitt, R. Saint and R. Schuh for providing antibodies. We are indebted to R. Reed for the use of the GFP dissecting microscope. Special thanks go to C. Comeaux for excellent technical assistance and E. Abrams for embryonic northern blots. P. L. B. is a Howard Hughes Medical Institute Predoctoral Fellow. Support for this research was provided by grant #RO1DE12873 from the National Institute of Dental and Craniofacial Research to Dr Andrew.

REFERENCES

Adams, M. D., Celniker, S. E., Holt, R. A., Evans, C. A., Gocayne, J. D., Amanatides, P. G., Scherer, S. E., Li, P. W., Hoskins, R. A., Galle, R. F. et al. (2000). The genome sequence of *Drosophila melanogaster*. *Science* **287,** 2185-2195.

Affolter, M., Nellen, D., Nussbaumer, U. and Basler, K. (1994). Multiple requirements for the receptor serine/threonine kinase *thick veins* reveal novel functions of TGF β homologs during *Drosophila* embryogenesis. *Development* **120,** 3105-3117.

Affolter, M. and Shilo, B. Z. (2000). Genetic control of branching morphogenesis during *Drosophila* tracheal development. *Curr. Op. Cell Bio.* **12,** 731-735.

Anderson, M. G., Perkins, G. L., Chittick, P., Shrigley, R. J. and Johnson, W. A. (1995). *drifter*, a *Drosophila* POU-domain transcription factor, is required for correct differentiation and migration of tracheal cells and midline glia. *Genes Dev.* **9,** 123-137.

Andrew, D. J., Baig, A., Bhanot, P., Smolik, S. M. and Henderson, K. D. (1997). The *Drosophila dCREB-A* gene is required for dorsal/ventral patterning of the larval cuticle. *Development* **124,** 181-193.

Andrew, D. J., Horner, M. A., Petitt, M. G., Smolik, S. M. and Scott, M. P. (1994). Setting limits on homeotic gene function: restraint of *Sex combs reduced* activity by *teashirt* and other homeotic genes. *EMBO J.* **13,** 1132-1144.

Bardwell, V. J. and Treisman, R. (1994). The POZ domain: a conserved protein-protein interaction motif. *Genes Dev.* **8,** 1664-1677.

Baumann, P. and Skaer, H. (1993). The *Drosophila* EGF receptor homologue (DER) is required for Malpighian tubule development. *Development* **Supplement**, 65-75.

Bienz, M. (1994). Homeotic genes and positional signalling in the *Drosophila* viscera. *Trends Genet.* **10,** 22-26.

Bier, E., Jan, L. Y. and Jan, Y. N. (1990). *rhomboid*, a gene required for dorsoventral axis establishment and peripheral nervous system development in *Drosophila melanogaster*. *Genes Dev.* **4,** 190-203.

Blake, K. J., Myette, G. and Jack, J. (1998). The products of *ribbon* and *raw* are necessary for proper cell shape and cellular localization of nonmuscle myosin in *Drosophila*. *Dev. Biol.* **203,** 177-188.

Blake, K. J., Myette, G. and Jack, J. (1999). *ribbon*, *raw*, and *zipper* have distinct functions in reshaping the *Drosophila* cytoskeleton. *Dev. Genes Evol.* **209,** 555-559.

Boube, M., Llimargas, M. and Casanova, J. (2000). Cross-regulatory interactions among tracheal genes support a co-operative model for the induction of tracheal fates in the *Drosophila* embryo. *Mech. Dev.* **91,** 271-278.

Brand, A. H. and Perrimon, N. (1993). Targeted gene expression as a means of altering cell fates and generating dominant phenotypes. *Development* **118,** 401-415.

Burge, C. and Karlin, S. (1997). Prediction of complete gene structures in human genomic DNA. *J. Mol. Biol.* **268,** 78-94.

Campos-Ortega, J. A. and Hartenstein, V. (1985). *The Embryonic Development of Drosophila melanogaster.* Berlin/Heidelberg: Springer-Verlag.

Casso, D., Ramirez-Weber, F. A. and Kornberg, T. B. (1999). GFP-tagged balancer chromosomes for *Drosophila melanogaster*. *Mech. Dev.* **88,** 229-232.

Chen, C. K., Kuhnlein, R. P., Eulenberg, K. G., Vincent, S., Affolter, M. and Schuh, R. (1998). The transcription factors KNIRPS and KNIRPS RELATED control cell migration and branch morphogenesis during *Drosophila* tracheal development. *Development* **125,** 4959-4968.

Chen, W., Zollman, S., Couderc, J. and Laski, F. (1995). The BTB domain of bric à brac mediates dimerization in vitro. *Mol. Cell. Biol.* **15,** 3424-3429.

Chihara, T. and Hayashi, S. (2000). Control of tracheal tubulogenesis by Wingless signaling. *Development* **127,** 4433-4442.

Franc, N. C., Heitzler, P., Ezekowitz, R. A. and White, K. (1999). Requirement for Croquemort in phagocytosis of apoptotic cells in *Drosophila*. *Science* **284,** 1991-1994.

Gabay, L., Seger, R. and Shilo, B. Z. (1997). MAP kinase in situ activation atlas during *Drosophila* embryogenesis. *Development* **124,** 3535-3541.

Gertler, F. B., Comer, A. R., Juang, J. L., Ahern, S. M., Clark, M. J., Liebl, E. C. and Hoffmann, F. M. (1995). *enabled*, a dosage-sensitive suppressor of mutations in the *Drosophila* Abl tyrosine kinase, encodes an Abl substrate with SH3 domain-binding properties. *Genes Dev.* **9,** 521-533.

Gregory, S. L., Kortschak, R. D., Kalionis, B. and Saint, R. (1996). Characterization of the *dead ringer* gene identifies a novel, highly conserved family of sequence-specific DNA-binding proteins. *Mol. Cell. Biol.* **16,** 792-799.

Hamilton, B. A. and Zinn, K. (1994). From clone to mutant gene. *Methods Cell Biol.* **44,** 81-94.

Harrison, S. D. and Travers, A. A. (1990). The *tramtrack* gene encodes a Drosophila finger protein that interacts with the *ftz* transcriptional regulatory region and shows a novel embryonic expression pattern. *EMBO J.* **9,** 207-216.

Henderson, K. D. and Andrew, D. J. (2000). Regulation and function of *Scr*, *exd*, and *hth* in the *Drosophila* salivary gland. *Dev. Biol.* **217,** 362-374.

Henderson, K. D., Isaac, D. D. and Andrew, D. J. (1999). Cell fate specification in the *Drosophila* salivary gland: the integration of homeotic gene function with the DPP signaling cascade. *Dev. Biol.* **205,** 10-21.

Jack, J. and Myette, G. (1997). The genes *raw* and *ribbon* are required for proper shape of tubular epithelial tissues in *Drosophila*. *Genetics* **147,** 243-253.

Kerber, B., Fellert, S. and Hoch, M. (1998). Seven-up, the *Drosophila* homolog of the COUP-TF orphan receptors, controls cell proliferation in the insect kidney. *Genes Dev.* **12,** 1781-1786.

Konsolaki, M. and Schupbach, T. (1998). *windbeutel*, a gene required for dorsoventral patterning in *Drosophila*, encodes a protein that has homologies to vertebrate proteins of the endoplasmic reticulum. *Genes Dev.* **12,** 120-131.

Kosman, D., Small, S. and Reinitz, J. (1998). Rapid preparation of a panel of polyclonal antibodies to *Drosophila* segmentation proteins. *Dev. Genes Evol.* **208,** 290-294.

Kuhnlein, R. P., Frommer, G., Friedrich, M., Gonzalez-Gaitan, M., Weber, A., Wagner-Bernholz, J. F., Gehring, W. J., Jackle, H. and Schuh, R. (1994). *spalt* encodes an evolutionarily conserved zinc finger protein of novel structure which provides homeotic gene function in the head and tail region of the *Drosophila* embryo. *EMBO J.* **13,** 168-179.

Kuhnlein, R. P. and Schuh, R. (1996). Dual function of the region-specific homeotic gene *spalt* during *Drosophila* tracheal system development. *Development* **122,** 2215-2223.

Kuo, Y. M., Jones, N., Zhou, B., Panzer, S., Larson, V. and Beckendorf, S. K. (1996). Salivary duct determination in *Drosophila*: roles of the EGF receptor signalling pathway and the transcription factors Fork head and Trachealess. *Development* **122,** 1909-1917.

Lehmann, R. and Tautz, D. (1994). In situ hybridization to RNA. In *Drosophila melanogaster*: *Practical Uses in Cell and Molecular Biology* (ed. L. S. B. Goldstein and E. A. Fyrberg), pp. 755. San Diego, CA: Academic Press, Inc.

Llimargas, M. (2000). Wingless and its signalling pathway have common and separable functions during tracheal development. *Development* **127,** 4407-4417.

Llimargas, M. and Casanova, J. (1997). Ventral veinless, a POU domain transcription factor, regulates different transduction pathways required for tracheal branching in *Drosophila*. *Development* **124,** 3273-3281.

Llimargas, M. and Casanova, J. (1999). EGF signalling regulates cell invagination as well as cell migration during formation of tracheal system in *Drosophila*. *Dev. Genes Evol.* **209,** 174-179.

Manning, G. and Krasnow, M. (1993). Tracheal Development. In *The Development of Drosophila melanogaster* (ed. M. Bate and A. Martinez Arias), pp. 609-685. Cold Spring Harbor: Cold Spring Harbor Laboratory Press.

McEwen, D. G., Cox, R. T. and Peifer, M. (2000). The canonical Wg and JNK signaling cascades collaborate to promote both dorsal closure and ventral patterning. *Development* **127,** 3607-3617.

Melnick, A., Ahmad, K. F., Arai, S., Polinger, A., Ball, H., Borden, K. L., Carlile, G. W., Prive, G. G. and Licht, J. D. (2000). In-depth mutational analysis of the promyelocytic leukemia zinc finger BTB/POZ domain reveals motifs and residues required for biological and transcriptional functions. *Mol. Cell. Biol.* **20,** 6550-6567.

Müller, S. A., Sasaki, T., Bork, P., Wolpensinger, B., Schulthess, T., Timpi, R., Engel, A. and Engel, J. (1999). Domain organization of Mac-2 binding protein and its oligomerization to linear and ring-like structures. *J. Mol. Biol.* **291,** 801-813.

Myat, M. M. and Andrew, D. J. (2000). Organ shape in the *Drosophila* salivary gland is controlled by regulated, sequential internalization of the primordia. *Development* **127,** 679-691.

Myat, M. M., Isaac, D. D. and Andrew, D. J. (2000). Early genes required for salivary gland fate determination and morphogenesis in *Drosophila melanogaster*. *Adv. Dental Res.* **14**, 89-98.

Noselli, S. and Agnes, F. (1999). Roles of the JNK signaling pathway in *Drosophila* morphogenesis. *Curr. Opin. Genet. Dev.* **9,** 466-472.

Nüsslein-Volhard, C., Wieschaus, E. and Kluding, H. (1984). Mutations affecting the pattern of the larval cuticle in *Drosophila melanogaster*. I. Zygotic loci on the second chromosome. *Roux's Arch. Dev. Biol.* **193,** 267-282.

Pardue, M. L. (1994). Looking at polytene chromosomes. *Methods Cell Biol.* **44,** 333-351.

Patel, N. H. (1994). Imaging neuronal subsets and other cell types in whole-mount *Drosophila* embryos and larvae using antibody probes. In *Drosophila melanogaster: Practical Uses in Cell and Molecular Biology* (ed. L. S. B. Goldstein and E. A. Fyrberg), pp. 445-487. San Diego: Academic Press.

Peifer, M., Orsulic, S., Pai, L. M. and Loureiro, J. (1993). A model system for cell adhesion and signal transduction in *Drosophila*. *Development* **Supplement** 163-176.

Raz, E. and Shilo, B. Z. (1993). Establishment of ventral cell fates in the *Drosophila* embryonic ectoderm requires DER, the EGF receptor homolog. *Genes Dev.* **7,** 1937-1948.

Reuter, R., Panganiban, G. E., Hoffmann, F. M. and Scott, M. P. (1990). Homeotic genes regulate the spatial expression of putative growth factors in

the visceral mesoderm of *Drosophila* embryos. *Development* **110,** 1031-1040.

Riesgo-Escovar, J. R. and Hafen, E. (1997). *Drosophila* Jun kinase regulates expression of *decapentaplegic* via the ETS-domain protein Aop and the AP-1 transcription factor DJun during dorsal closure. *Genes Dev.* **11,** 1717-1727.

Robinson, D. N. and Cooley, L. (1997). *Drosophila* Kelch is an oligomeric ring canal actin organizer. *J. Cell Biol.* **138,** 799-810.

Rorth, P., Szabo, K., Bailey, A., Laverty, T., Rehm, J., Rubin, G. M., Weigmann, K., Milan, M., Benes, V., Ansorge, W. and Cohen, S. M. (1998). Systematic gain-of-function genetics in *Drosophila*. *Development* **125,** 1049-1057.

Ruberte, E., Marty, T., Nellen, D., Affolter, M. and Basler, K. (1995). An absolute requirement for both the type II and type I receptors, Punt and Thick veins, for Dpp signaling in vivo. *Cell* **80,** 889-897.

Rubin, G. M. and Spradling, A. C. (1983). Vectors for P element-mediated gene transfer in *Drosophila*. *Nucleic Acids Res.* **11,** 6341-6351.

Sakai, T., Wada, T., Ishiguro, S. and Okada, K. (2000). RPT2: A signal transducer of the phototropic response in Arabidopsis. *Plant Cell* **12,** 225-236.

Samakovlis, C., Hacohen, N., Manning, G., Sutherland, D. C., Guillemin, K. and Krasnow, M. A. (1996). Development of the *Drosophila* tracheal system occurs by a series of morphologically distinct but genetically coupled branching events. *Development* **122,** 1395-1407.

Shiga, Y., Tanaka-Matakatsu, M. and Hayashi, S. (1996). A nuclear GFP/β-galactosidase fusion protein as a marker for morphogenesis in living *Drosophila*. *Develop. Growth Differ.* **38,** 99-106.

Skaer, H. and Martinez Arias, A. (1992). The *wingless* product is required for cell proliferation in the malpighian tubule anlage of *Drosophila melanogaster*. *Development* **116,** 745-754.

Sutherland, D., Samakovlis, C. and Krasnow, M. A. (1996). *branchless* encodes a *Drosophila* FGF homolog that controls tracheal cell migration and the pattern of branching. *Cell* **87,** 1091-1101.

Szuts, D., Eresh, S. and Bienz, M. (1998). Functional intertwining of Dpp and EGFR signaling during *Drosophila* endoderm induction. *Genes Dev.* **12,** 2022-2035.

Szuts, D., Freeman, M. and Bienz, M. (1997). Antagonism between EGFR and Wingless signalling in the larval cuticle of *Drosophila*. *Development* **124,** 3209-3219.

Tearle and Nüsslein-Volhard, C. (1987). Tubingen mutants and stock list. *DIS* **66,** 209-269.

Thompson, J. D., Gibson, T. J., Plewniak, F., Jeanmougin, F. and Higgins, D. G. (1997). The CLUSTALX windows interface: flexible strategies for multiple sequence alignment aided by quality analysis tools. *Nucleic Acids Res.* **25,** 4876-4882.

Vincent, S., Ruberte, E., Grieder, N. C., Chen, C. K., Haerry, T., Schuh, R. and Affolter, M. (1997). DPP controls tracheal cell migration along the dorsoventral body axis of the *Drosophila* embryo. *Development* **124,** 2741-2750.

Wan, S., Cato, A. M. and Skaer, H. (2000). Multiple signalling pathways establish cell fate and cell number in *Drosophila* malpighian tubules. *Dev. Biol.* **217,** 153-165.

Wappner, P., Gabay, L. and Shilo, B. Z. (1997). Interactions between the EGF receptor and DPP pathways establish distinct cell fates in the tracheal placodes. *Development* **124,** 4707-4716.

Wodarz, A., Grawe, F. and Knust, E. (1993). CRUMBS is involved in the control of apical protein targeting during *Drosophila* epithelial development. *Mech. Dev.* **44,** 175-187.

Young, P. E., Richman, A. M., Ketchum, A. S. and Kiehart, D. P. (1993). Morphogenesis in *Drosophila* requires nonmuscle myosin heavy chain function. *Genes Dev.* **7,** 29-41.